Architectural Disparity Effects in the Morphology of Dendrimer−Linear Coil Diblock Copolymers

Darrin J. Pochan* and Lisa Pakstis

Materials Science and Engineering and Delaware Biotechnology Institute, University of Delaware, Newark, Delaware 19716

Elbert Huang

IBM T. J. Watson Research Center, P.O. Box 218, Yorktown Heights, New York 10958

Craig Hawker and Robert Vestberg

IBM Almaden Research Center, 650 Harry Road, San Jose, California 95120

John Pople

Stanford Linear Accelerator Center, Stanford Synchrotron Radiation Laboratory, Stanford, California 94309

Received May 16, 2002
Revised Manuscript Received August 27, 2002

Diblock copolymers with extreme architectural asymmetry, namely dendritic−linear coil molecules, have recently been exploited in the construction of well-defined Langmuir−Blodgett monolayers[1] and the chemical alteration of bulk material surfaces via adsorption.[2] Others have studied the assembly of dendritic−linear hybrid blocks in aqueous solution for solute encapsulation.[3] These studies of supramolecular assembly and surface adsorption/assembly exploit the high density of chemical functionality on the periphery of dendritic molecules and the disparate chemical nature inherent in block copolymers for structure formation via self-assembly from solution. To understand the effects of the architectural asymmetry present in dendritic−linear coil block copolymers on supramolecular self-assembly and structure formation, the bulk phase behavior of two series of benzyl ether dendrimer−polystyrene (PS) linear coil diblocks was characterized.

Recent work has focused on the effects of molecular graft architecture on bulk block copolymer phase-separated morphology.[4−6] It has been shown that A_nB star molecules form traditional block copolymer phases but at significantly higher relative volume fractions of B to A than observed in linear diblocks.[7−10] The crowding of *n* arms of A at the AB interface forces the interfacial curvature toward the B block to alleviate chain stretching of A and to provide significant interfacial volume to the crowded A arms.[11] A comparison to star or miktoarm[4] block copolymers is not completely rigorous due to the lack of significant chain stretching in dendritic molecules. However, the interfacial volume required to pack the dendrimer blocks in a phase-separated domain is a significant factor relative to the linear coil block and will force the linear PS to reside on the concave interface up to significantly higher relative block compositions than observed in linear diblocks.

The synthesis of diblock copolymers comprised of linear polystyrene (PS) and benzyl ether dendrimer blocks is reported elsewhere.[12] Molecular characteristics of the fifth- and sixth-generation dendrimer/PS block copolymers are listed in Table 1 along with the respective characterized morphology. The molecules are designated by the benzyl ether dendrimer block generation number followed by the dendrimer weight fraction. The molecular weight of the dendrimeric block was calculated from its chemical structure, and the PS molecular weight is approximated from the increase in total molecular weight of the block copolymer as determined by GPC.

It has been previously demonstrated that block copolymer systems that microphase separate into well-defined morphologies normally exhibit island/hole structures with topographies that equal the natural domain spacing of the morphology, *d*. This results from a combination of effects stemming from surface-induced alignment[13] and commensurability of the natural domain spacing with film thickness.[14,15] To utilize this phenomenon as a simple means to monitor the ordering behavior of these systems, films with thicknesses of ∼50−150 nm were cast onto Si substrates and annealed at 170 °C for 12 h under a nitrogen purge. The films were first examined by optical microscopy whereby island/hole topographies were clearly evident in many of the systems as abrupt color changes corresponding with a discrete variation in film thickness were observed. AFM was used to measure the step heights of these topographies to obtain the domain periodicity, *d*. Examples of AFM images obtained for samples 5-37 and 6-38 are shown in Figure 1, and the results from these studies are tabulated in Table 1.

Small-angle X-ray scattering was also used to monitor the ordering behavior in films melt-pressed at 170 °C. The data were circularly averaged, and two representative SAXS plots are shown in Figure 2 for samples 5-37 and 6-38 where the intensity, *I*, is plotted as a function of the scattering wave vector, *q*. The domain periodicity, *d*, obtained from Bragg's law $d = 2\pi/q_{max}$ was calculated for each sample and is tabulated in Table 1. These results are in excellent agreement with the AFM results. Neglecting effects from morphology, these results are consistent with the general expectation that the domain periodicity scales with the total molecular weight of the block copolymer as the domain periodicity increases with molecular weight of the PS block and, for comparable weight fractions of dendrimer, are larger for the G6 systems.

Characterization of the microphase-separated bulk morphologies was further accomplished with transmission electron microscopy (TEM). Sections with thickness <100 nm were microtomed for TEM at room temperature with a diamond knife and then stained for 30 min in a closed chamber by exposure to a 4% RuO_4 aqueous solution atmosphere. While RuO_4 reacts with both blocks of the block copolymer, the benzyl ether dendritic block stained more strongly than the linear PS, thus providing significant electron density contrast in bright field imaging. A JEOL 2000FX TEM equipped with a LaB_6 filament was used at 200 kV accelerating voltage for bright field imaging. TEM results representative of the G5 and G6 sample series are shown in Figure 3.

A significant molecular architecture effect on the resultant phase-separated morphologies relative to what is observed in linear diblock copolymers[16,17] is apparent, most noticeably in the G6 diblocks. G6-51 exhibits a PS

10.1021/ma0207531 CCC: $22.00
Published on Web 10/15/2002

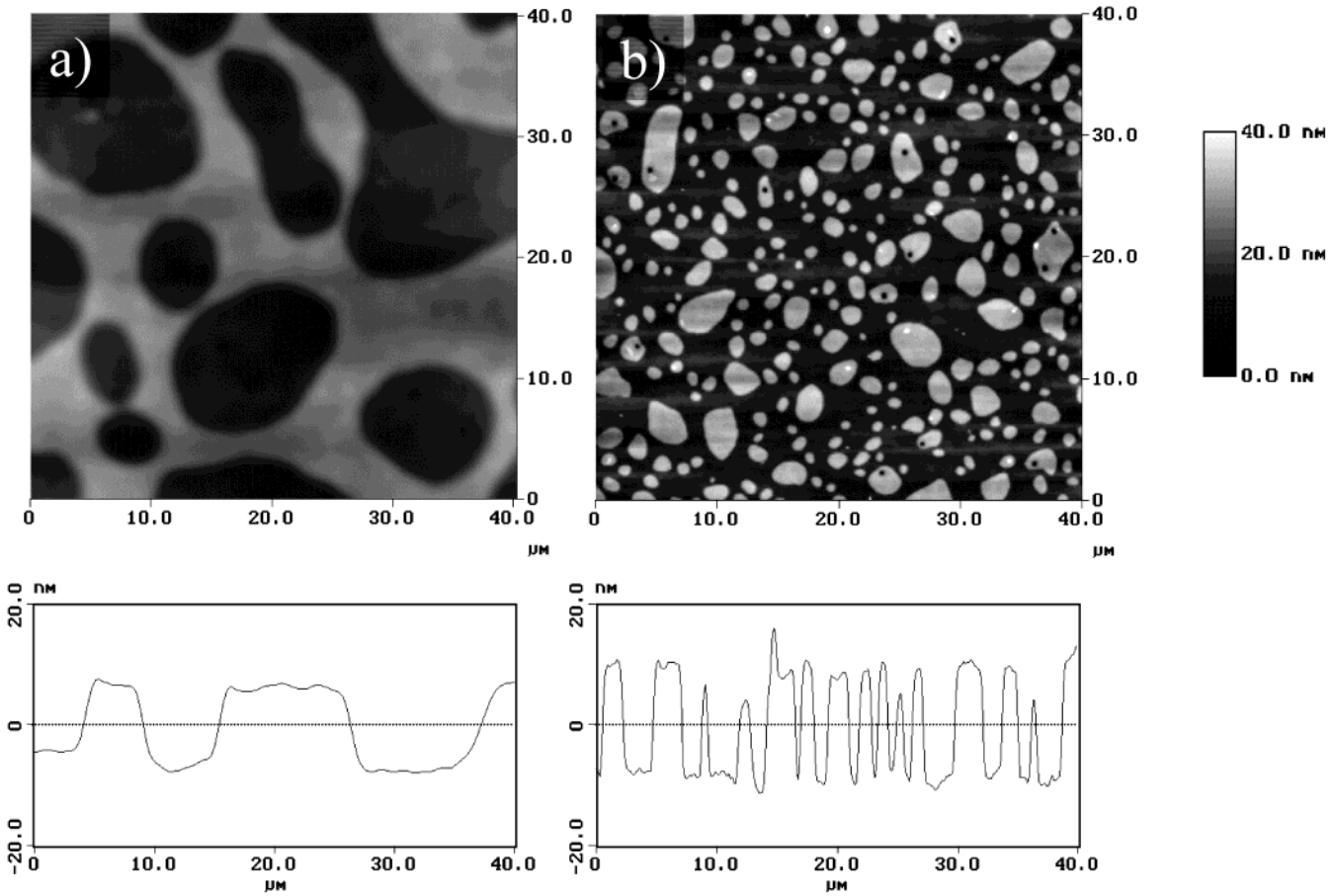

Figure 1. Typical height contrast AFM images obtained on annealed block copolymer films for samples (a) G5-37 and (b) G6-38.

Table 1. Molecular Characteristics and Bulk Morphology

designation (generation no. − dendrimer wt %)	dendrimer	M_W (PS) (10^3 g/mol)	wt % dendrimer	total M_W (10^3 g/mol)	d (Å) (SAXS)	d (Å) (AFM)	morphology (TEM)
5-37	G5	11.3	37.1	18.0	129	127	NA
5-24	G5	21.1	24.0	27.8	152	147	phase-separated/disordered
5-13	G5	45.0	12.9	51.7	180	NA	phase-separated/disordered
5-7	G5	89.9	6.9	96.6	213	NA	phase-separated/disordered
6-51	G6	12.8	51.3	26.3	162	168	cylindrical
6-38	G6	22.1	37.8	35.6	193	191	lamellar
6-22	G6	48.5	21.7	62.0	240	257	disrupted lamellae
6-12	G6	97.0	12.2	110.5	252	NA	phase-separated/disordered
6-6	G6	217.2	5.8	230.7	314	NA	phase-separated/disordered

cylindrical phase despite the symmetric volume fraction of the two blocks. In contrast, a phase-separated linear diblock copolymer system would be centrally located in the lamellar region of the phase diagram. G6-38 is clearly a lamellar structure while linear blocks of this same relative volume fraction would reside on the lamellar/perforated lamellar/bicontinuous/cylindrical phase boundaries depending on slight differences in chain flexibility and/or molecular weight.[17,18]

The morphology of G6-22 displays the most interesting effects of the linear−dendritic architecture. While a linear diblock would exhibit minority component cylinders, the local linear−dendritic morphology is a lamellar-like structure. Tilting experiments perpendicular to the long axis of the layers revealed no hexagonal symmetry, confirming the local alternating layered structure. The alternating layers seem to be frustrated from persisting for more than several hundred angstroms in the layer plane before consequently pinching off, forming ubiquitous, varied defects. Defined grain structure is not observed in the sample despite a clear, local layered phase separation. This lamellar frustration can be attributed to the inability of the noninterpenetrating dendrimer blocks to pack on a concave interface; i.e., the system still preferred a flat interfacial curvature but was forced to pinch off the lamellae frequently due to the overwhelming majority volume fraction component PS. Only in G6-12 were the stained dendritic blocks finally forced to the concave interface, forming disordered, spherical domains. A specific lattice packing of the dendrimer block minority phase domains was frustrated despite the small volume fraction of dendritic block. The remaining G6 sample, G6-6, formed a similar disordered spherical domain morphology and is not presented.

It should be noted that the morphologies characterized herein are consistent with independently characterized structure on the same class of sixth-generation benzyl ether dendritic−PS linear coil diblocks with different relative ratios of block components presented by Mackay et al.[12] At 31 wt % dendrimer they observed lamellae while at 18 wt % dendrimer cylinders of the

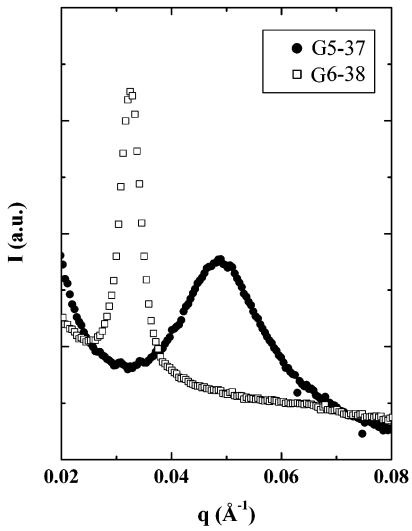

Figure 2. Circularly averaged SAXS intensity plotted as a function of the scattering wave vector, q, comparing the long spacing observed in similar dendrimer block fractions in both fifth- and sixth-generation dendrimer blocks, samples G5-37 and G6-38. Only low scattering vector, q (where $q = (4\pi/\lambda)\sin(\theta/2)$, θ is the scattering angle and λ is the X-ray wavelength of 1.488 Å), is shown since no higher order peaks were observed in the azimuthally integrated data. All other samples exhibited similar behavior—the long spacings observed for all samples are tabulated in Table 1.

dendritic blocks were observed. In this work lamellae are observed down to 22 wt % dendrimer while at 12 wt % a random phase-separated structure is observed. Our observations do not preclude the presence of a dendrimer cylinder phase at dendrimer fractions between 12 and 22 wt %. However, within the context of the independent experimental observations presented here, when ≤12 wt % the dendrimer block is not observed to reside on a concave interface *and concurrently* produce a well-ordered lattice of a specific minority domain shape. Furthermore, the solution-casting sample preparation in Mackay et al. may produce more long-range ordered grains of a particular morphology at a specific relative block weight percent than the melt pressing sample preparation used here but should not produce a completely different morphology and lattice symmetry.

Despite the low molecular weights of the relatively symmetric G6-51 and G6-38 diblocks (Table 1) and the low χ parameter between PS and the benzyl ether dendrimer building blocks ($\sim 10^{-4}$ as estimated from solubility parameters in Mackay et al.[12]), the series is well within the strongly segregated phase-separated regime as evidenced by the large grains of regular phase-separated nanostructure in G6-51 and G6-38. For this to be true, there must be a large entropic component to the interaction parameter due to the large conformational asymmetry between the dendritic and linear blocks (as also proposed in Mackay et al.[12]). In addition to altering the morphological behavior in strongly segregated systems,[18−20] conformational asymmetry has been experimentally and theoretically observed to contribute significantly to the thermodynamic interactions between polyolefinic blocks,[21,22] specifically making them less compatible than predicted solely through enthalpic interactions. With our limited survey of relative block fractions and overall molecular weights, it is unclear whether the phase-separated but disordered

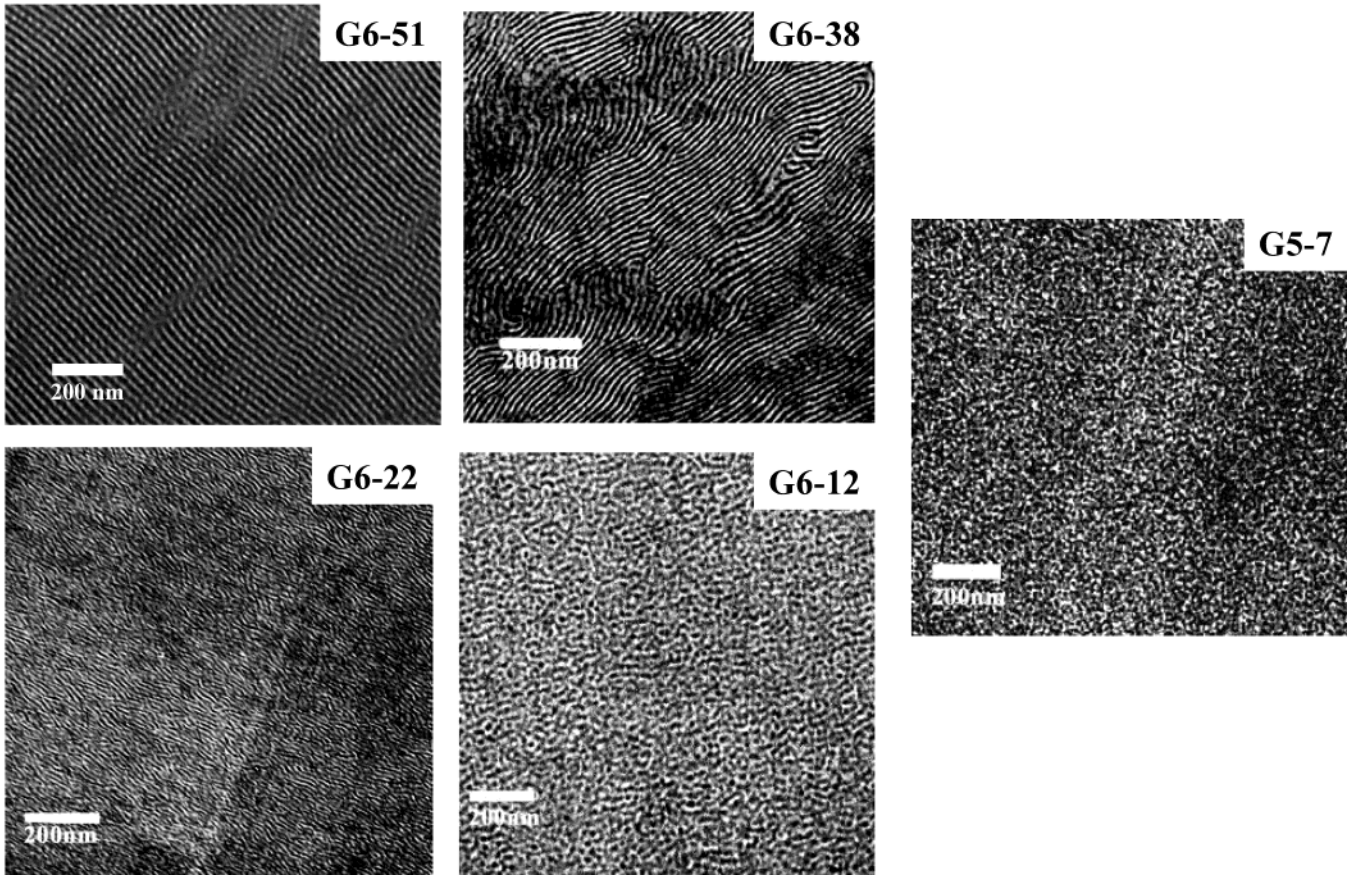

Figure 3. Transmission electron micrographs of RuO_4-stained, microphase-separated sixth- and fifth-generation benzyl ether dendrimer (dark regions)—polystyrene (light regions) diblock copolymers.

structures observed in the highly asymmetric blocks (G6-22, G6-12) are due to weakly segregated thermodynamics or to the frustration of dendrimer packing on a concave interface in the bulk. All G6 samples that show a regular microphase-separated morphology in the bulk exhibit ordered film formation behavior with well-defined holes and islands, an example of which is shown in Figure 1. The long spacings of the phase-separated structure as determined from the hole depth/island height are commensurate with those observed in the bulk.

In contrast, the entire G5 block copolymer series formed locally phase-separated structures lacking both long-range lattice formation and a regular local domain structure, similar to what is observed in weakly segregated block copolymer systems.[23] A representative image is shown in Figure 3 for the sample G5-7. By significantly lowering the molecular weight of the dendritic block (from $\sim 13.4 \times 10^3$ g/mol in the G6 series to $\sim 6.4 \times 10^3$ g/mol), the G5 series appears to no longer reside in the strongly segregated regime. In particular, G5-37 and G5-24 (18.0×10^3 and 27.8×10^3 g/mol, respectively) are disordered while similar dendrimer fractions at larger molecular weight in G6-38 and G6-22 (35.6×10^3 and 62.0×10^3 g/mol, respectively) are clearly well ordered in the bulk. Interestingly, when confined to a two-dimensional thin film G5-37 and G5-24 ordered into well-defined films with quantized islands and holes, indicating a well-ordered phase-separated morphology. This behavior is consistent with surface-induced phase separation and ordering of block copolymer films previously observed in linear molecules.[24]

In conclusion, significant deviations are observed in the relationship of morphology to relative block fraction in comparison to linear diblock copolymers. The extreme contrast in architecture between the two blocks shifts the morphology phase boundaries to significantly higher volume fractions of the linear coil block so that the dendrimers can reside on a convex or flat interface. Therefore, the architectural asymmetry present in dendritic−linear coil block copolymers is a useful molecular parameter in the design of new self-assembling, microphase-separated materials.

Acknowledgment. The authors gratefully acknowledge partial support from the NSF Center for Polymeric Interfaces and Macromolecular Assemblies (CPIMA) under cooperative agreement DMR-9400354 and the American Chemical Society Petroleum Research Fund under award PRF# 35577-G7. In addition, the authors acknowledge the support of the Stanford Synchrotron Radiation Laboratory in providing the facilities in which the small-angle X-ray scattering measurements were performed.

References and Notes

(1) Johnson, M. A.; Santini, C. M. B.; Iyer, J.; Satija, S.; Ivkov, R.; Hammond, P. T. *Macromolecules* **2002**, *35*, 231−238.
(2) Frechet, J. M. J.; Gitsov, I.; Monteil, T.; Rochat, S.; Sassi, J. F.; Vergelati, C.; Yu, D. *Chem. Mater.* **1999**, *11*, 1267−1274.
(3) Gitsov, I.; Lambrych, K. R.; Remnant, V. A.; Pracitto, R. *J. Polym. Sci., Part A: Polym. Chem.* **2000**, *38*, 2711−2727.
(4) Pitsikalis, M.; Pispas, S.; Mays, J. W.; Hadjichristidis, N. *Adv. Polym. Sci.* **1998**, *135*, 1−137.
(5) Beyer, F. L.; Gido, S. P.; Buschl, C.; Iatrou, H.; Uhrig, D.; Mays, J. W.; Chang, M. Y.; Garetz, B. A.; Balsara, N. P.; Tan, N. B.; Hadjichristidis, N. *Macromolecules* **2000**, *33*, 2039−2048.
(6) Hasegawa, H.; Hashimoto, T.; Hyde, S. T. *Polymer* **1996**, *37*, 3825−3833.
(7) Pochan, D. J.; Gido, S. P.; Pispas, S.; Mays, J. W.; Ryan, A. J.; Fairclough, J. P. A.; Hamley, I. W.; Terrill, N. J. *Macromolecules* **1996**, *29*, 5091−5098.
(8) Tselikas, Y.; Iatrou, H.; Hadjichristidis, N.; Liang, K. S.; Mohanty, K.; Lohse, D. J. *J. Chem. Phys.* **1996**, *105*, 2456−2462.
(9) Beyer, F. L.; Gido, S. P.; Velis, G.; Hadjichristidis, N.; Tan, N. B. *Macromolecules* **1999**, *32*, 6604−6607.
(10) Yang, L. Z.; Hong, S.; Gido, S. P.; Velis, G.; Hadjichristidis, N. *Macromolecules* **2001**, *34*, 9069−9073.
(11) Milner, S. T. *Macromolecules* **1994**, *27*, 2333−2335.
(12) (a) Hay, G.; Mackay, M. E.; Hawker, C. J. *J. Polym. Sci., Part B: Polym. Phys.* **2001**, *39*, 1766−1777. (b) Mackay, M.; Hong, Y.; Jeong, M.; Tande, B.; Wagner, N.; Hong, S.; Gido, S.; Vestberg, R.; Hawker, C. *Macromolecules* **2002**, *35*, 8391−8399.
(13) Anastasiadis, S. H.; Russell, T. P.; Satija, S. K.; Majkrzak, C. F. *J. Chem. Phys.* **1990**, *92*, 5677−5691.
(14) Anastasiadis, S. H.; Russell, T. P.; Satija, S. K.; Majkrzak, C. F. *Phys. Rev. Lett.* **1989**, *62*, 1852−1855.
(15) Coulon, G.; Russell, T. P.; Deline, V. R.; Green, P. F. *Macromolecules* **1989**, *22*, 2581−2589.
(16) Matsen, M. W.; Bates, F. S. *Macromolecules* **1996**, *29*, 1091−1098.
(17) Bates, F. S.; Fredrickson, G. H. *Annu. Rev. Phys. Chem.* **1990**, *41*, 525−557.
(18) Matsen, M. W.; Bates, F. S. *J. Polym. Sci., Part B: Polym. Phys.* **1997**, *35*, 945−952.
(19) Pochan, D. J.; Gido, S. P.; Zhou, J.; Mays, J. W.; Whitmore, M.; Ryan, A. J. *J. Polym. Sci., Part B: Polym. Phys.* **1997**, *35*, 2629−2643.
(20) Chen, J. T.; Thomas, E. L.; Ober, C. K.; Mao, G. P. *Science* **1996**, *273*, 343−346.
(21) Gehlsen, M. D.; Bates, F. S. *Macromolecules* **1994**, *27*, 3611−3618.
(22) Fredrickson, G. H.; Liu, A. J.; Bates, F. S. *Macromolecules* **1994**, *27*, 2503−2511.
(23) Hashimoto, T.; Sakamoto, N.; Koga, T. *Phys. Rev. E* **1996**, *54*, 5832−5835.
(24) Mansky, P.; Tsui, O. K. C.; Russell, T. P.; Gallot, Y. *Macromolecules* **1999**, *32*, 4832−4837.

MA0207531